SLEEPJ, 2019, 1–16

doi: 10.1093/sleep/zsy244
Advance Access Publication Date: 11 December 2018
Original Article

ORIGINAL ARTICLE

Direct activation of G-protein-gated inward rectifying K+ channels promotes nonrapid eye movement sleep

Bende Zou[1], William S. Cao[1], Zhiwei Guan[2], Kui Xiao[1], Conrado Pascual[1], Julian Xie[1], Jingxi Zhang[1], James Xie[1], Frank Kayser[1], Craig W. Lindsley[3], C. David Weaver[3], Jidong Fang[2] and Xinmin (Simon) Xie[1,*]

[1]AfaSci Research Laboratories, Redwood City, CA, [2]Department of Psychiatry, Pennsylvania State University College of Medicine, Hershey, PA and [3]Department of Pharmacology, Vanderbilt University, Nashville, TN

*Corresponding author. Xinmin (Simon) Xie, AfaSci Research Laboratories, 522 Second Avenue, Redwood City, CA 94063. Email: simonxie@afasci.com.

Abstract

Study Objectives: A major challenge in treating insomnia is to find effective medicines with fewer side effects. Activation of G-protein-gated inward rectifying K^+ channels (GIRKs) by $GABA_B$ agonists baclofen or γ-hydroxybutyric acid (GHB) promotes nonrapid eye movement (NREM) sleep and consolidates sleep. However, baclofen has poor brain penetration, GHB possesses abuse liability, and in rodents both drugs cause spike-wave discharges (SWDs), an absence seizure activity. We tested the hypothesis that direct GIRK activation promotes sleep without inducing SWD using ML297, a potent and selective GIRK activator.

Methods: Whole-cell patch-clamp recordings from hypocretin/orexin or hippocampal neurons in mouse brain slices were made to study neuronal excitability and synaptic activity; spontaneous activity, locomotion, contextual and tone-conditioned memory, and novel object recognition were assessed. Electroencephalogram/electromyogram (EEG/EMG) recordings were used to study GIRK modulation of sleep.

Results: ML297, like baclofen, caused membrane hyperpolarization, decreased input resistance, and blockade of spontaneous action potentials. Unlike baclofen, ML297 (5–10 μM) did not cause significant depression of postsynaptic excitatory and inhibitory currents (EPSCs–IPSCs), indicating preferential postsynaptic inhibition. ML297 (30 mg/kg, i.p.) inhibited wake activity and locomotion, and preferentially increased NREM sleep without altering EEG delta power, REM sleep, inducing SWDs, or impairing conditioned memory and novel object recognition.

Conclusions: This study finds that direct activation of neuronal GIRK channels modulates postsynaptic membrane excitability and prolongs NREM sleep without changing sleep intensity, inducing SWDs, or impairing memory in rodents. These results suggest that direct GIRK activation with a selective compound may present an innovative approach for the treatment of chronic insomnia.

Statement of Significance

Multiple neurotransmitters binding to G-protein-coupled receptors activate G-protein-gated inwardly rectifying K^+ (GIRK) channels, thereby moderating neuronal excitability and neurotransmission. Baclofen and γ-hydroxybutyric acid binding to $GABA_B$ receptors activate GIRK channels and enhance nonrapid eye movement (NREM) sleep in humans and rodents, but also cause side effects possibly associated with receptor distribution and presynaptic modulation via effectors other than GIRK channels. Here we find that direct activation of neuronal GIRK channels with ML297 mimics sleep promotion, particularly enhancing NREM sleep like $GABA_B$ agonists, but without inducing spike-wave discharges, an absence seizure activity, or causing memory impairment. The present study suggests that direct GIRK channel activation with a selective compound can provide a new approach to treat chronic insomnia.

Key words: G-protein-gated inwardly rectifying potassium channels; hippocampus; hypothalamus; ML297; patch clamp recording; sleep

Submitted: 1 March, 2018; **Revised:** 16 November, 2018
© Sleep Research Society 2018. Published by Oxford University Press on behalf of the Sleep Research Society.
All rights reserved. For permissions, please e-mail journals.permissions@oup.com.

Downloaded from https://academic.oup.com/sleep/article-abstract/42/3/zsy244/5238085 by Law Library user on 06 April 2019

Introduction

Reduced total sleep time and quality are widespread modern phenomena. Many factors affect sleep quantity and quality including shift work, travel, sound, lighting, noise level, and particularly stress. Collectively, these factors cause various sleep disorders. Insomnia is the most prevalent type of sleep disorder, affecting 25%–30% of adults worldwide, and its incidence increases with age [1]. Moreover, insomnia extends into the pediatric population, presenting an increasing and significant health issue [2]. There is hardly an area of health that is not adversely affected by sleep disturbances [1]. Chronic insomnia not only decreases alertness and performance, but also negatively influences mental and physical health. Chronic sleep disturbances are associated with cardiometabolic diseases, psychiatric disorders, and all-cause mortality [3]. Chronic insomnia is well-known to be associated with obesity, diabetes, anxiety, depression, and chronic pain [1]. Recently, an overwhelming number of studies further link chronic insomnia to Alzheimer's disease, Parkinson disease, posttraumatic stress disorder, and substance abuse [4–8]. Insomnia in the elderly is a risk factor for Alzheimer's disease and amyloid-beta levels in the brain are increased with prolonged wakefulness [9, 10]. The association of sleep disturbance with posttraumatic stress disorder and substance use disorders is seen in both humans [11] and animals [12]. Poor sleep quality predicts later relapse across different addictive drugs including nicotine, alcohol, cocaine, amphetamines, and opioids [13]. More than one third of opioid addicts report poor sleep as a reason for relapse [14, 15].

Insomnia with these comorbidities responds poorly to pharmacotherapy [16] and, in many cases, is refractory to current hypnotic medications such as benzodiazepines, nonbenzodiazepines, the melatonin receptor agonist ramelteon, histamine H_1 receptor antagonists, and antidepressants [17, 18]. Suvorexant, a dual orexin receptor A and B antagonist, provides a new mechanism of action in the treatment of insomnia [19–21]. Although most of these medications help us to induce sleep, few of them selectively increase nonrapid eye movement (NREM) sleep or consolidate sleep, which are considered more desirable. Baclofen and γ-hydroxybutyric acid (GHB) can promote NREM sleep; however, baclofen has poor brain penetration and dose-limiting side effects while GHB has a short half-life ($t_{1/2}$ < 30 min) and abuse liability. Neither drug is suitable for the treatment of chronic insomnia. There is a need for new and better insomnia therapeutics that can promote sleep, especially NREM sleep, with fewer side effects [22, 23].

To explore a new sleep-promoting target and potential therapeutic, we took a novel approach by directly activating G-protein-gated inward rectifying K^+ (GIRK) channels using our recently discovered selective GIRK channel direct activator ML297 [24]. GIRK channels are comprised of four subunits (1–4 or K_{ir}3.1–3.4). Different compositions of homo- and hetero-tetrameric GIRK channels display organ-specific, brain region-specific, and cell type-specific localization (e.g. hippocampal neurons predominantly contain GIRK1/2, whereas cardiac myocytes contain GIRK1/4) [25, 26]. GIRK channels are partially and constitutively activated by a variety of endogenous neurotransmitters acting through the βγ subunits of $G_{i/o}$-coupled G-protein-coupled receptors, for example γ-aminobutyric acid (GABA) acting on $GABA_B$ receptors. Exogenous drugs such as baclofen and GHB bind to the $GABA_B$ receptors [27] and activate GIRK channels; this predominantly increases NREM sleep or slow-wave sleep and improves sleep continuity in humans and rodents [28–31]. Direct GIRK channel activation should produce similar NREM sleep promotion while bypassing receptor activation pathways. Therefore, this approach may reduce unwanted side effects associated with $GABA_B$ receptor activation due to its wide distribution and presynaptic inhibitory modulation via other effectors such as N-type Ca^{2+} channels. To test this hypothesis, we took advantage of the small molecule probe ML297, a potent and selective GIRK channel activator [24]. Our multidisciplinary approach consisted of in vitro patch-clamp recording and electroencephalogram/electromyogram (EEG/EMG) recording techniques, as well as in vivo neurobehavioral assessment. We have demonstrated that direct activation of GIRK channels with ML297 selectively causes postsynaptic inhibition with minimal depression of presynaptic neurotransmission and preferentially increases NREM sleep without inducing spike-wave discharges (SWDs), an abnormal electrical brain activity frequently induced by overactivation of $GABA_B$ receptors with baclofen or GHB in rodents [32–34]. Moreover, we demonstrated that ML297 at an effective sleep-promoting dose (30 mg/kg) did not cause memory impairment in mice using the contextual- and tone-fear conditioning test and a novel object recognition (NOR) assessment.

Methods

Experimental animals

Animal studies were approved by the Institutional Animal Care and Use Committees of AfaSci Research Laboratories and were performed in conformance with the US Public Health Service Guidelines on Care and Use of Animals in Research. The orexin/enhanced green fluorescent protein (EGFP) transgenic mice, in which EGFP is expressed exclusively in orexin neurons in C57BL/6 mouse background [35], were from breeding colonies. Wild-type mice (C57BL/6) and rats (Sprague Dawley) were purchased from Envigo (Placentia, CA). The animals were group-housed in homecages under standard environmental conditions (24°C–26°C; 12/12 [light/dark] hr cycle). Food and water were provided ad libitum.

Electrophysiological recordings

Mice (both sexes, 20–40 days old) were anesthetized with isoflurane and decapitated. The brain was quickly removed and placed into ice-cold artificial cerebrospinal fluid (ACSF) that was continuously bubbled with 5% CO_2/95% O_2. The ACSF consisted of (in mM): NaCl (130), $MgCl_2$ (2), KCl (3), $CaCl_2$ (1), HEPES-Na (10), and glucose (10). The hypothalamic brain slices (from orexin/EGFP transgenic mice) and hippocampal brain slices (from wild-type mice) for patch clamp recordings were cut in coronal section at 250 μm thickness using a vibratome (Leica VT100S, Leica Biosystems, Inc., Buffalo Grove, IL). Slices were incubated in ACSF continuously bubbled with 5% CO_2/95% O_2 for at least 1 hr before transfer to the recording chamber. The slices were recorded within 6 hr after dissection at room temperature (22°C–25°C).

EGFP-labeled hypocretin neurons in hypothalamic slices were visually identified using a fluorescence microscope and whole-cell current-clamp recordings were performed. CA1 pyramidal

Downloaded from https://academic.oup.com/sleep/article-abstract/42/3/zsy244/5238085 by Law Library user on 06 April 2019

neurons in hippocampal slices were identified and whole-cell voltage-clamp recordings were performed. Recordings were performed using the MultiClamp 700B amplifier and analyzed offline with pCLAMP10.4 software (Molecular Devices, San Jose, CA). The external ACSF solution was perfused at a rate of 2–2.5 mL/min by gravity and the recording chamber volume was approximately 0.4 mL. The recording electrode was filled with the internal solution consisting of (in mM) the following: K-Gluconate (140), K-EGTA (1), $CaCl_2$ (0.1), $MgSO_4$ (2), HEPES (10), ATP-Mg (2), and GTP-Mg (0.5). The recording electrodes had resistances of 3–4 Mega-ohms (MΩ) in the bath solution. Whole-cell patch recordings had series resistances of <25 MΩ after whole-cell configuration and were periodically checked with the seal test voltage step (10 mV, 10 ms) to monitor series resistances throughout the recordings. Hyperpolarizing current pulses (–0.3 nA, 500 ms) were delivered every 5 s throughout the experiment, unless otherwise specified, to monitor membrane input resistance as described previously [36]. Liquid junction potentials of –10.9 ± 0.6 mV (n = 6) were measured using an Ag/AgCl reference electrode with 3 M KCl concentration. All resting or holding potentials in our whole-cell recordings were corrected with the measured junction potential. The stimulation electrode (FHC, Inc., Bowdoin, ME) was placed in the Schaffer collateral and commissural fibers of the hippocampal slice to record the excitatory postsynaptic current (EPSC). In a specific EPSC experiment, a small and brief hyperpolarizing voltage step (5 mV, 2 ms) was applied 5 ms prior to the synaptic stimulation to monitor membrane conductance and access resistance changes. To record the monosynaptic inhibitory postsynaptic current (IPSC), the electrode was placed in the stratum radiatum close to the recorded neuron to directly stimulate interneurons.

Neurobehavioral assessment

Mouse (C57BL/6, male, approximately 3 months old) spontaneous activity (active/inactive state), locomotion (travel distance, velocity, and movement trajectories), and rearing, an exploring behavior, in its homecage were monitored using a noninvasive monitor—the SmartCage system [37] (AfaSci, Inc., Redwood City, CA). The system consists of 22 infrared (IR) photo-beam sensors and is flexibly integrated with modular devices (e.g. footshock device for fear-conditioning learning and memory test, and rotarod device for rotarod performance). Homecage activity was determined by beam breaks (x-, y-, and z-axis photo-beam break counts). Data were automatically analyzed using the CageScore program (AfaSci, Inc.) [37]. Distance traveled in centimeters was obtained from the lower horizontal sensors (3 cm apart in x-axis and 2 cm apart in y-axis) taking into account the path taken. Average velocity was computed as distance traveled/second in the forward direction, and rearing activity was detected by an upper row of IR sensors (5 cm in z-axis above the lower IR sensors). Inactive state occurs when the animal blocks only 1 or 2 adjacent low row of IR sensors and does not block the upper IR row. Animals were monitored for 2–6 days under normal 12/12 (light/dark) hr cycles (light on 7 am and off at 7 pm). After accommodation toward stable activity, the drug solution or vehicle (0.5% hydroxyl propyl cellulose aqueous solution containing 2% dimethyl sulfoxide, DMSO) was administered via intraperitoneal injection (i.p.) 5–10 min prior to the onset of the dark phase and recordings continued for 24 or more hours. The behavioral parameters as a function of recording time were plotted in 1 or 2 hr blocks. Righting reflex was conducted in the same cohort of mice after completion of homecage monitoring by random assignment into two groups (n = 8/group). Time taken to turn over from a dorsal position and four paws righting up was measured 30 min posttreatment with ML297 (30 mg/kg, i.p.) or vehicle using a stop watch.

Rotarod test

For rotarod testing, a three-lane rotarod modular device was inserted within the SmartCage platform. Individual mice were placed on the rod within the lane and then rod rotation was controlled by the behavior monitoring system at a selected speed (a constant speed mode at a fixed 20 rpm). When the test subject fell off the rod, the event was detected by the IR sensors and the amount of time the subject stayed on the rod was automatically recorded by the system. Two groups of mice from the same cohort of animals used in the righting reflex test (n = 8 mice/group) were trained on rotarod performance over 4 consecutive days. On training days, each mouse was allowed to perform on the rotarod a total of 3 times. Time on the rod was averaged and plotted as a function of days in a time course. After completion of training on day 4, one group received an injection of ML297 (100 mg/kg, i.p.), whereas the other group received vehicle. Approximately 30 min after drug/vehicle injection, each mouse's rotarod performance was assessed 3 times and time on the rod was averaged for each mouse.

EEG/EMG recordings and sleep analysis

Adult mice (C57BL/6, male, 25–30 g, 2.5–3 months old, n = 11) were implanted with EEG electrodes on the right cerebral hemisphere over the frontal and parietal cortices. EMG electrodes were implanted into the muscle of the dorsal neck. The animals were given a 2 week recovery and a 4 day adaptation period to the recording environment as well as a headstage-cable system before experiments. Throughout the recovery and experimental periods, the animals were maintained on a 12/12 (light/dark) hr cycle with food and water freely available. The EEG and EMG signals were amplified and filtered with a Grass Neurodata Model 12 Amplifier system (Grass Instrument Division of Astro-Med, Inc., West Warwick, RI). The EEG signals were filtered with low and high cutoffs at 0.3 and 30.0 Hz, respectively. The EMG signals and motor activity signals were filtered with low and high cutoffs at 100 and 300 Hz, respectively. The analog outputs of the amplified signals were digitized at 128 Hz for EEG and 256 Hz for EMG. In addition, global activity was detected with a piezoelectric sensor and its amplified signals were digitized through the same analog-to-digital (A/D) converter (USB-2533, Measurement Computing, Norton, MA) as used for EEG/EMG and saved to the hard drive of a personal computer. The SleepWave program (Biosoft Studio, Hershey, PA) was used for recording and data analysis [38, 39].

EEG and EMG, and piezoelectric activity signals were simultaneously recorded for at least 24 hr after vehicle or drug treatment. Under our experimental conditions, both EEG/EMG recordings were stable. Since the biological $t_{1/2}$ of ML297 is relatively short (approximately 20 min) [40, 41], animals could fully recover from the drug action. We therefore tested vehicle (i.p.) as baseline and ML297 at 10 and 30 mg/kg (i.p.) in the same subjects on different days (with 1 week separation between

Downloaded from https://academic.oup.com/sleep/article-abstract/42/3/zsy244/5238085 by Law Library user on 06 April 2019

the two doses) at a similar circadian time with all injections made 5–10 min before dark onset. Sequential 4 s segments of EEG, EMG, and EEG power spectra were graphically displayed with the SleepWave software and manually scored as described previously [38, 39]. Wakefulness was identified by low EEG amplitude with high and variable EMG signals. Rapid eye movement (REM) sleep was identified by low amplitude EEG dominated by θ activity (5–10 Hz in rodents) and the absence of muscle tone with occasional muscle twitches. NREM sleep was identified by slow- and high-amplitude EEG and low-amplitude EMG. EEG signals within each 4 s segment were subjected to fast-Fourier transformation (FFT) analysis yielding power spectra between 0.5 and 30.0 Hz, with a 0.5 Hz frequency resolution after treatment with Hann window in 2 s, and then averaged every 4 s using three overlapping 2 s windows. The three vigilant states in 1 hr bins were plotted as a function of Zeitgeber time (ZT).

The EEG power spectra during NREMS were analyzed in different frequency bands (δ, 0.5–4.0 Hz; θ, 0.45–8.0 Hz, α, 8.5–12.5 Hz; and β, 12.5–30.0 Hz) by normalizing to the mean baseline as 100% (24 hr after vehicle injection). EEG power spectra in 6 hr bins were analyzed and plotted as a function of ZT.

In addition, EEG/EMG recordings were made in male Sprague Dawley rats (300–500 g) following a similar surgical operation, recovery, and recording procedures. The EEG recorded for 4–6 hr during the light phase. The SWD scoring criteria were based on the EEG activity described in the literature [32–34]. Typically each SWD consists of 4–7 Hz large amplitude brain electrical waveforms lasting for 3–5 s.

Contextual- and tone-conditioning fear tests

Mice (C57BL/6, male, approximately 3 months old) were subjected to footshock fear-conditioning on the training day using the footshock module (AfaSci, Inc.), which consists of a metal grid and an electric stimulation generator controlled by the behavior monitor system. On the training day, each mouse's locomotion and rearing activity were recorded for 5 min as the baseline followed by five mild electric footshocks to the paws via the metal grid (each stimulus was 70 ± 2 V, 2 s, delivered at a 60 s interval). Each footshock (unconditioned stimulus) was paired with a tone (conditioned stimulus or cue). The tone preceded the shock by 2 s and lasted for a total of 6 s. ML297 (30 mg/kg, i.p.) was administrated 30–40 min prior to memory testing at 24 hr after the training.

Two types of memory tests were conducted. First, the contextual fear-conditioning test [42] was performed by placing the test subject onto the metal grid in the footshock chamber where behavior was recorded for 5 min. The setting was identical to that of the training day but without shocks and tones. Freezing behavior, an indicator of a fear response in rodents, was classified based on a criterion that the animal stays in an inactive status (without movement and rearing) constantly for a defined duration (>2–10 s used in the literature [42, 43]). The CageScore program has an adjustable freezing time threshold (default 10 s). Freezing level was quantified by total freezing time (in s), percentage (%), and number (#) in a 5 min test period. In this study, freezing percentage at baseline prior to footshocks and in memory test 24 hr after footshocks were compared to assess the contextual fear retention.

Next, tone-conditioning fear responses were assessed immediately after the contextual fear test for each mouse. The mouse was transferred into a fresh normal homecage (without bedding) and its locomotion and rearing activity were recorded by the behavior monitor for 15 min. The initial 5 min recording without tones served as the baseline and the subsequent 5 min had 5 tones (without shock) to induce cued fear response. As rodents naturally accommodate to a new environment, their activity gradually decreases; the last 5 min of recovery activity after the tone served to verify the tone-conditioned fear response. The locomotion and rearing activity before, during, and after tones in 1 min time bins and freezing percentage in each 5 min block were plotted to assess tone-conditioned fear response.

Novel object recognition

NOR test was conducted in a separate cohort of mice (C57BL/6, male, approximately 3 months old) to evaluate recognition memory which is based on the spontaneous tendency of mice to spend more time exploring a novel object relative to a familiar one [44]. The NOR test is performed in an open field arena (43.2 × 43.2 × 30.5 cm) with two different objects, A and B, that are consistent with respect to height and volume, but differ in shape and appearance. On the training/learning day prior to memory testing day, mice are first habituated to the open field arena by allowing exploration of the empty arena for 10 min. After habituation, individual animals were exposed to two identical objects, A and A′, which were spaced diagonally across two of the corners of the open field. Mice were allowed to explore the objects for 10 min and the duration spent investigating each of the identical objects was scored. The mice were then removed from the arena and returned to their original homecage. Baseline exploration (%) of each object was calculated by exploration time of A or A′ divided by total exploration time of A and A′ using the following formula:

$$[\text{A or A'}/(\text{A} + \text{A'})] * 100\%.$$

Following 24 hr after training and 30 min postdrug/vehicle injection (i.p.), the individual mice were returned to the arena containing the familiar object A and the novel object B, and allowed to explore for 10 min. The time spent investigating each object was scored. Memory ability was measured using the following formula:

$$[\text{B}/(\text{A} + \text{B})] * 100\%$$

A complete failure of memory results in a ≤50% Exploration of B and higher % Exploration of B reflects better memory. The total time spent exploring both objects on the training day controls for baseline arousal level, interest in investigating objects, and potential bias. On the memory testing day, the total time exploring both objects can also reflect alertness and potential drug effects on locomotion.

Drugs

ML297 was synthesized at the Vanderbilt Institute of Chemical Biology, Vanderbilt University, (Nashville, TN) or at the Department of Pharmacology, University of California, Davis (Davis, CA). R-baclofen, CGP52432, diazepam, and bicuculline were purchased from Sigma-Aldrich (St Louis, MO), and γ-butyrolactone (GBL) from Spectrum (New Brunswick, NJ). For

Downloaded from https://academic.oup.com/sleep/article-abstract/42/3/zsy244/5238085 by Law Library user on 06 April 2019

in vitro experiments, all drugs were made in stock solution with DMSO and freshly diluted with the external recording solutions to the final concentrations (0.01%–0.1% DMSO) for bath-application via perfusion at a 2 mL/min flow rate. For in vivo tests, ML297 was initially dissolved in DMSO and then diluted with 0.5% hydroxypropyl cellulose aqueous solution. Final drug solutions, as well as the vehicle, contained 2% DMSO and intraperitoneal injection volume was 10 mL/kg of body weight.

Statistical analysis

In all behavior tests and scoring, the researchers were blinded to treatments. All data are presented as mean ± SEM. For experiments involving two groups, paired or unpaired *t*-tests were used as appropriate. For experiments involving more than two groups with two factors (treatment and time), two-way analysis of variance (ANOVA) for repeated measures was used for overall comparisons. If significant differences were found for the main effects or interactions, post hoc analyses using Fisher's protected least significant difference (PLSD) test, or Tukey test, were conducted. Data were analyzed using Excel, GraphPad Prism (version 5.0, GraphPad Software, San Diego, CA), and StatView (version 5.0.1, SAS Institute, Inc., Cary, NC). The significance level for the two-sided analysis was set at $p < 0.05$.

Results

ML297 directly activates GIRK channels preferentially producing postsynaptic inhibition without depression of presynaptic neurotransmission

Arousal, wakefulness, and sleep are controlled by the interaction between excitatory and inhibitory neuronal activity in the brain. The hypocretin system has been recognized to play an architectural role in wake/sleep state regulation, whereas hippocampal pyramidal neurons contribute to alertness, cognitive behavior, and indirectly modulate wake/sleep. We therefore studied direct GIRK channel activation in wake/sleep regulation by investigating cellular electrophysiological effects of ML297 on these two types of excitatory neurons. Modulation of hypocretin neurons by ML297 was evaluated using whole-cell current-clamp recordings of visually identified hypocretin neurons from orexin/EGFP transgenic hypothalamic brain slices. The bath-application of ML297 (10 μM) caused long-lasting hyperpolarization (–9 ± 1 mV, $n = 4$), decreased input resistance (43 ± 4% of control), and blocked spontaneous firing of action potentials in hypocretin neurons (Figure 1A). The concentration-dependent hyperpolarizing response to ML297 in hypocretin neurons reveals a half-maximal efficacy concentration (EC_{50}) of 5.4 μM (Figure 1B; each data point represents $n = 3$–5 cells). In the presence of the Na^+ channel blocker tetrodotoxin (TTX, 0.3 μM) to block action potentials and presynaptic neurotransmission, the current-voltage relationship of membrane response in the presence and absence of ML297 indicates the reversal potential of the ML297-induced response to be –84 ± 6 mV, which is close to the K^+ equilibrium potential under the experimental conditions (Figure 1C and D; $n = 11$).

Similar to its action on hypocretin neurons [45], R-baclofen (10 μM) caused long-lasting hyperpolarization (–11 ± 1 mV, $n = 3$), a decrease in input resistance (48 ± 8% of control), and blockade of spontaneous firing of action potentials of CA1 neurons in hippocampal brain slices from wild-type mice (Figure 1E). $GABA_B$ receptor activation-induced responses are well-known to be mediated through G-protein coupled receptor (GPCR)-GIRK channel signaling [46]. Like baclofen, ML297 (10 μM) produced similar responses of hyperpolarization (–9 ± 1 mV, $n = 4$), decreased input resistance (43 ± 4% of control), and blockade of spontaneous action potentials, which were reversibly blocked by $BaCl_2$, a general K^+ channel blocker (Figure 1F). In another CA1 neuron, in the presence of the $GABA_B$ receptor antagonist CGP52432 (10 μM) and TTX (0.3 μM), 10 μM R-baclofen-mediated postsynaptic responses were completely prevented. In contrast, application of ML297 (10 μM) produced hyperpolarization and decreased input resistance (Figure 1G), confirming ML297-induced responses through direct activation of GIRK channels and not via interacting with $GABA_B$ receptors.

To study the effects of ML297 on synaptic activity, we took advantage of the well-defined neuroanatomic structure of the hippocampal slice. Whole-cell recordings were performed under voltage-clamp mode to minimize the consequence of ML297-induced postsynaptic hyperpolarization. The EPSC recorded in the Schaffer collateral-CA1 synapses is a monosynaptic pathway [47]. As shown in the EPSC-time course (Figure 2A), the bath-application of R-baclofen (10 μM) for approximately 10 min substantially depressed the EPSC in the CA1 neuron. After washout of baclofen and subsequent application of ML297 (10 μM) for more than 10 min, the EPSC was not inhibited; rather, it was slightly increased. After washout of ML297, EPSCs were blocked by 6,7-dinitroquinoxaline-2,3-dione (DNQX, 10 μM), confirming its mediation via the α-amino-3-hydroxy-5-methyl-4-isoxazolepropionic acid (AMPA) receptor. Individual cells and group-averaged responses to drug treatment were plotted in Figure 2B–E, showing that the effects of ML297 and baclofen on the EPSC were apparently opposite.

Next, the effects of ML297 on IPSCs were examined. Unlike the excitatory monosynaptic pathway, inhibitory neurotransmission is polysynaptic in the hippocampal slice [47, 48]. To avoid indirect inhibition of IPSCs by ML297 resulting from its postsynaptic action on upstream modulatory neurons, monosynaptic IPSCs were evoked by local direct stimulation of interneurons in stratum radiatum close to the recorded CA1 pyramidal neuron as described previously [27]. Using this method, evoked outward IPSCs and drug effects were plotted as a function of time (Figure 2F). ML297 (10 μM) slightly inhibited the IPSC by 22 ± 6%. After washout of ML297, the subsequent application of R-baclofen (10 μM) almost completely blocked the IPSCs in a reversible manner. The recovered IPSC after washout of baclofen was completely abolished by the $GABA_A$ receptor antagonist bicuculline (20 μM), confirming $GABA_A$ receptor mediation (Figure 2G–J; $n = 5$).

ML297 decreases wakeful spontaneous activity, locomotion, and preferentially increases NREM sleep

Next, we studied behavioral endpoints resulting from cellular inhibition of neuronal excitability by direct GIRK channel activation. Using a noninvasive neurobehavioral monitoring system [37, 43, 49, 50], spontaneous activity (mainly indicated by travel distance and rearing) was used to quantify active/inactive status and drug effects on general behavior over a 6 day recording

Downloaded from https://academic.oup.com/sleep/article-abstract/42/3/zsy244/5238085 by Law Library user on 06 April 2019

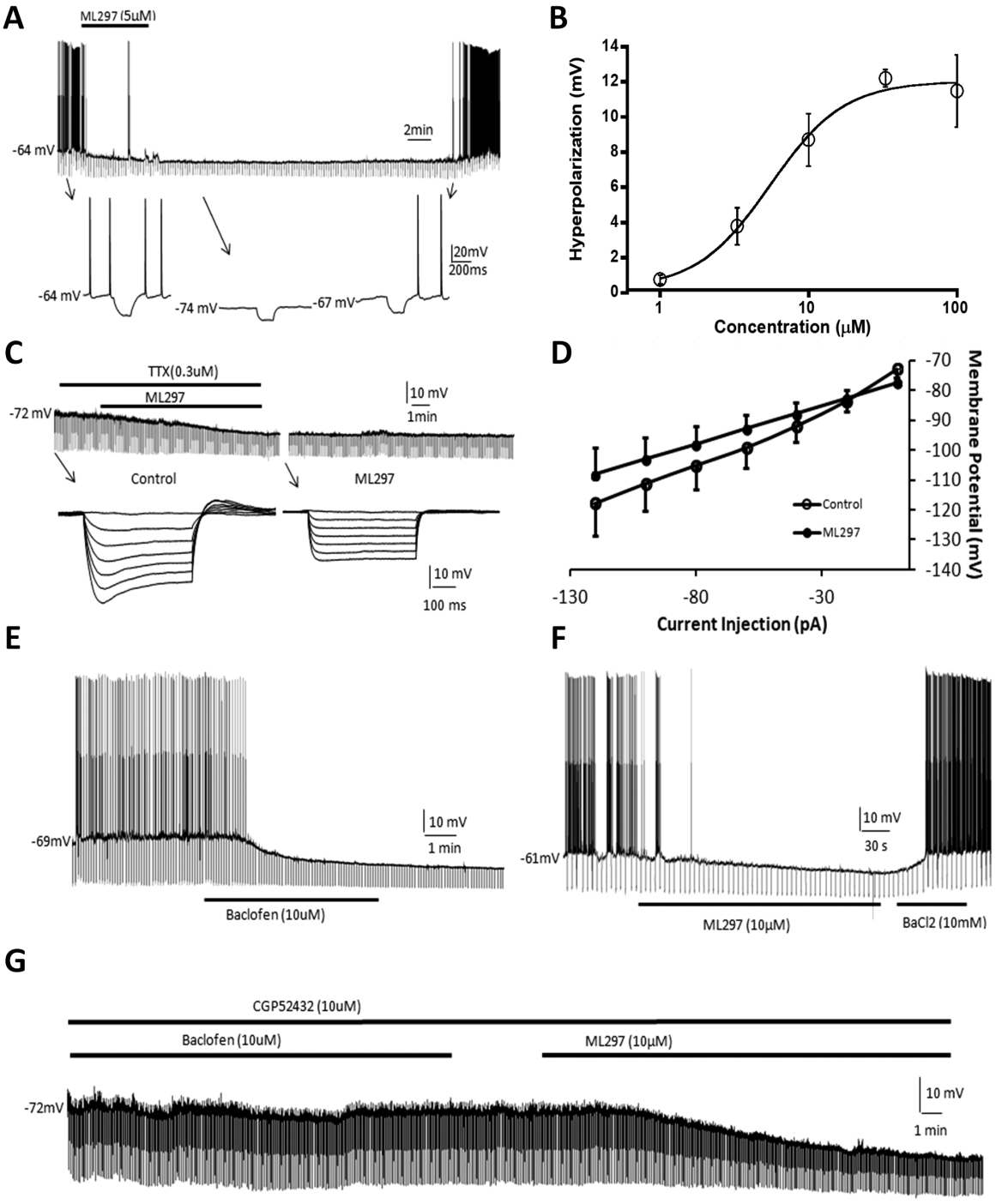

Figure 1. GIRK channel direct activation with ML297 causes hyperpolarization and a decrease in input resistance in hypothalamic hypocretin neuron and hippocampal CA1 neurons. (A) ML297 (5 μM) caused a long-lasting hyperpolarization, decreased input resistance, and blocked spontaneous firing of action potentials of a hypocretin neuron in the hypothalamic brain slice. Lower inserts indicated by arrows show time-expanded traces. (B) The concentration-dependent response curve of hyperpolarization by ML297 reveals an EC_{50} of 5.4 μM (each data point represents n = 3–5 cells). (C) In the presence of tetrodotoxin (0.3 μM), ML297 (5 μM) induced postsynaptic hyperpolarization and a decrease in input resistance. Lower inserts indicated by arrows show time-expanded traces. (D) Membrane potential changes in response to a series of current injections revealed a current-voltage relationship where the intersection point of the two current–voltage curves in the presence and absence of ML297 indicated a reversal potential of –84 mV (n = 11), which is close to the K^+ equilibrium potential and the experimental condition. (E) R-baclofen (10 μM) hyperpolarized a hippocampal pyramidal CA1 neuron by –12 mV, decreased input resistance to 40% of control level, and blocked spontaneous firing of action potentials. (F) ML297 (10 μM) induced similar postsynaptic responses as baclofen in another hippocampal CA1 neuron, which was reversibly blocked by $BaCl_2$ (10 mM), a general K^+ channel blocker. (G) In another CA1 neuron, in the presence of the $GABA_B$ antagonist CGP52432 and tetrodotoxin (TTX, 0.3 μM), R-baclofen (10 μM) did not induce any postsynaptic responses. Subsequent application of 10 μM ML297 induced responses of hyperpolarization and an increase in input resistance. Hyperpolarizing current pulses (–0.3 nA, 500 ms) were delivered every 5 s throughout the experiment in all recorded neurons which had resting potentials between –50 and –65 mV.

Downloaded from https://academic.oup.com/sleep/article-abstract/42/3/zsy244/5238085 by Law Library user on 06 April 2019

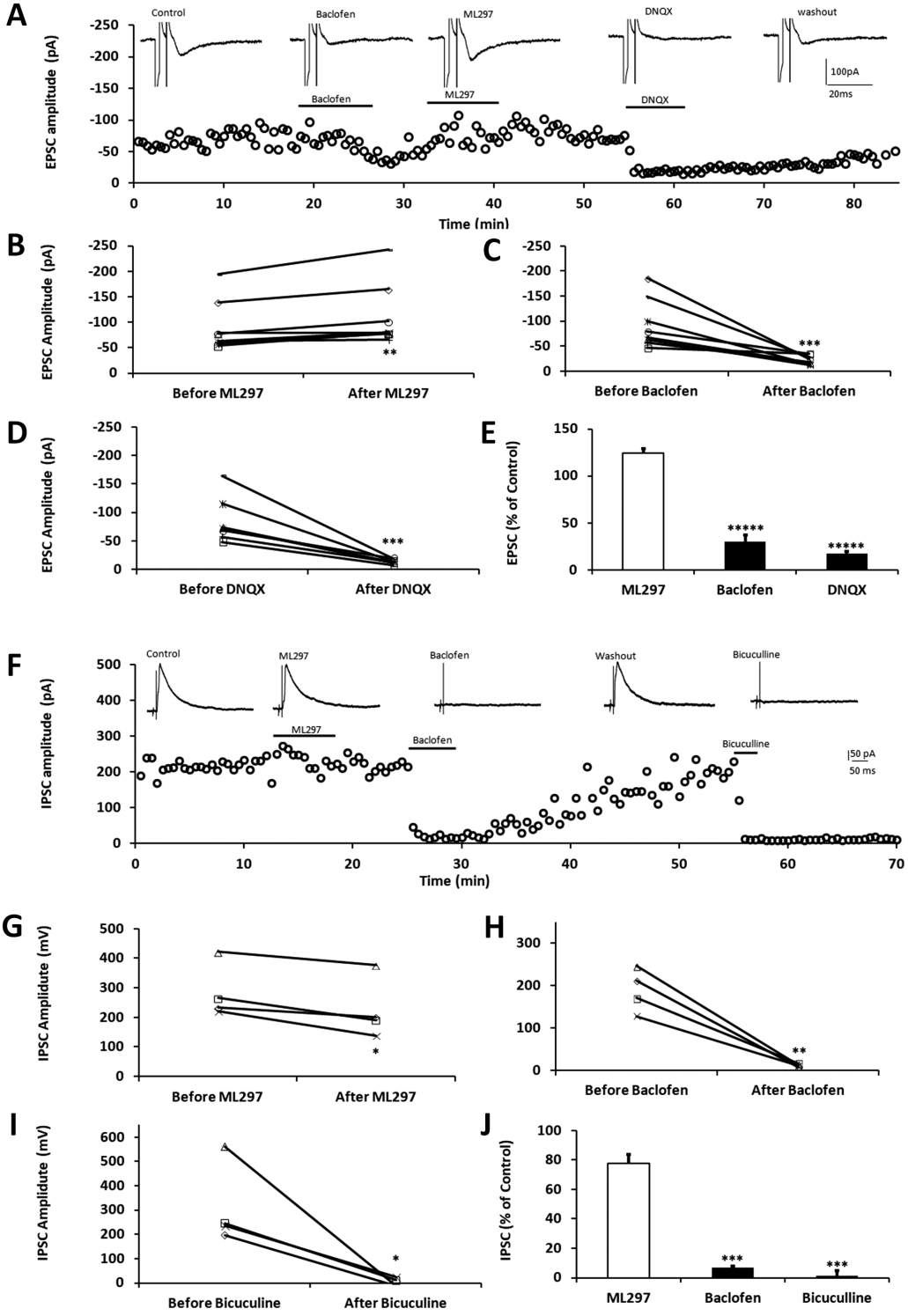

Figure 2. ML297 and R-baclofen produce differential modulation on EPSCs–IPSCs in hippocampal CA1 pyramidal neurons. (A) Perfusion of baclofen (10 μM) reversibly blocked the EPSC. After washout of baclofen, the recovered EPSCs were slightly increased by subsequent application of ML297 (10 μM), whereas DNQX (15 μM), a selective AMPA receptor antagonist, blocked the EPSCs at the end of the experiment. A small and brief hyperpolarizing voltage step (–5 mV, 2 ms) was applied prior to each synaptic stimulation to monitor membrane conductance and access resistance, which appeared to be consistent throughout the experiment. (B–E) Drug effects on EPSCs in individual cells and on group averaged responses were plotted (n = 8 per treatment; ANOVA, **** $p < 0.001$). The neurons were held at –60 mV and the Schaffer Collateral fibers were electrically stimulated at a 10 s interval. (F) In another group of CA1 neurons, perfusion of ML297 (10 μM) slightly inhibited IPSCs which were evoked by directly local stimulation to the interneurons close to the recorded pyramidal cells. Subsequent application of baclofen (10 μM) reversibly blocked the IPSCs. After washout of baclofen, the recovered IPSCs were completely inhibited by bicuculline (20 μM) in the same hippocampal neuron. (G–J) The graphs summarize drug effects on IPSCs in individual cells and on group averaged responses (n = 4 per treatment; ANOVA, *** $p < 0.01$). The neurons were held at –60 mV and local stimulation was delivered at a 10 s interval.

Downloaded from https://academic.oup.com/sleep/article-abstract/42/3/zsy244/5238085 by Law Library user on 06 April 2019

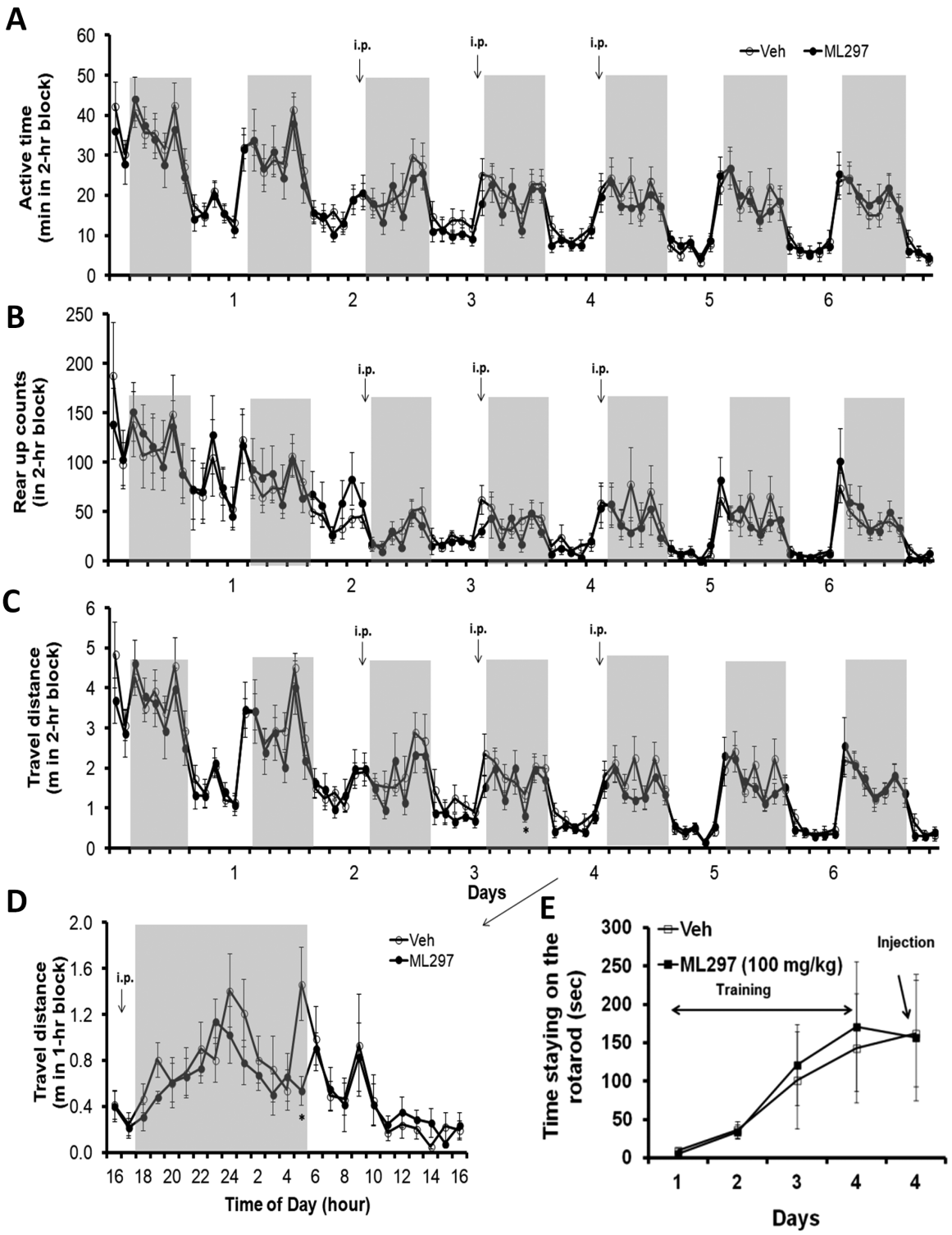

Figure 3. Effects of activation of GIRK channels with ML297 on mouse spontaneous activity, rearing, locomotion, and rotarod performance. Individual mice in fresh homecages that were placed within the SmartCage platforms were continuously monitored for 7 days under normal 12/12 (light/dark) hr cycle. The initial 2 days of recordings during accommodation to the new environment served as a baseline. Daily dosing of ML297 was performed (30 mg/kg, i.p.) 5–10 min prior to the dark onset on 3 consecutive days and animals were continually monitored for another 2 days of recovery after washout of the drug. (A) Active time calculated based on time spent in active state in 2 hr bins was plotted against days of recordings. (B) Rearing activity was measured by automatically counting rearing up episodes detected by the upper row of IR sensors. (C) Travel distance measured by integrating traveling distance along movement trajectories. (D) Travel distance taken from day 4 was plotted in 1 hr bins. All three key parameters indicate that ML297 reversibly reduced active time and inhibited mouse spontaneous activity in dark period. The asterisk * indicates $p < 0.05$ ($n = 8$ per group). The gray shadow indicates dark phase (light on 7 am and off at 7 pm). (E) The modular rotarod device was connected to and controlled by the behavior monitoring system. Time on the rotating rod was averaged and plotted as a function of days in a time course. After the last training on day 4, ML297 (100 mg/kg, i.p.) was administered in one group while another group received vehicle ($n = 8$/group).

Downloaded from https://academic.oup.com/sleep/article-abstract/42/3/zsy244/5238085 by Law Library user on 06 April 2019

period. Spontaneous activity gradually decreased as the animals accommodated to the environment of the monitoring platform. The first 2 days of recordings served as a baseline (Figure 3A–C). ML297 (30 mg/kg, i.p.) was administered daily at the onset of dark phase for 3 consecutive days and caused modest decreases in active time, travel distance, and rearing activity compared with their own baselines and to the vehicle control group in parallel monitoring. The travel distance on the second day of treatment with ML297 shown in 1 hr bins indicates a clear inhibition of locomotor activity, suggesting a sleep-promoting effect (Figure 3D).

Righting reflex was conducted in the same cohort of mice after completion of homecage monitoring. Time taken to turn over from a dorsal position and four paws righting up was measured 30 min postinjection. ML297 (30 mg/kg, i.p.)-treated mice displayed a righting reflex of <1 s, which was insignificant compared with the vehicle control ($n = 8$/group, unpaired Student t-test, $p > 0.05$). In contrast, ketamine (80 mg/kg, intramuscular injection) abolished righting reflex and caused unconsciousness.

To further assess drug effects on muscle coordination and balance, these two groups of mice were trained to perform on the rotarod controlled by the SmartCage system. As shown in Figure 3E, ML297 at 100 mg/kg (i.p.) did not significantly reduce the time spent on the rotating rod compared with its own performance in previous training trials prior to treatment with ML297 or to the vehicle injection control group.

Next, EEG/EMG signals and piezoelectric activity were simultaneously recorded to investigate the sleep-promoting effect of ML297. The representative traces of EEG and EMG recordings and wake/sleep state as a function of time shown in Figure 4 indicate that ML297 (30 mg/kg, i.p.) administered at the beginning of the dark phase mainly caused an increase in NREM sleep, whereas the EEG and EMG amplitudes were similar between vehicle control (baseline) and ML297 treatment in the same test subjects. Quantitative vigilant state analysis reveals that ML297 (10–30 mg/kg, i.p.) primarily increased NREM sleep time in a dose-related manner. ML297 at 10 mg/kg did not significantly alter the amounts of wakefulness, NREM

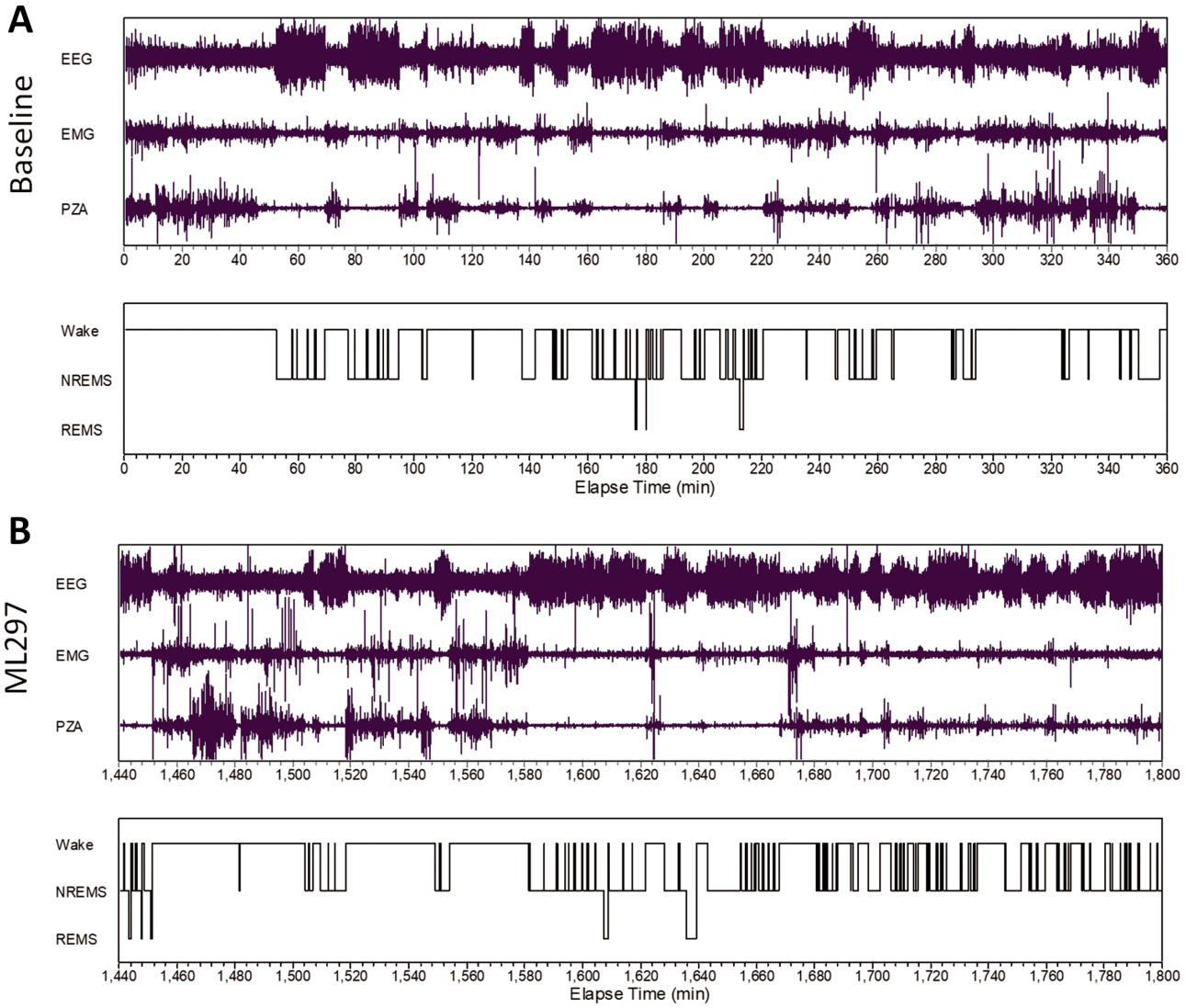

Figure 4. Representative EEG/EMG and piezoelectric (PZA) recordings from a rat. (A) Baseline of EEG/EMG and PZA signals was recorded after a vehicle injection and the analyzed vigilant states were plotted in as a function of recording time elapsed. (B) Following the administration of ML297 (30 mg/kg, i.p.), continued recordings of EEG/EMG and PZA signals and vigilant states were plotted in as a function of recording time.

Downloaded from https://academic.oup.com/sleep/article-abstract/42/3/zsy244/5238085 by Law Library user on 06 April 2019

sleep, or REM sleep (Figure 5A–C). At a higher dose of 30 mg/kg, ML297 produced a significant decrease in wakefulness (ANOVA, $F_{(1,10)} = 25.069$, $p < 0.001$) and an increase in NREM sleep ($F_{(1,10)} = 21.318$, $p < 0.001$), without changing REM sleep compared with the vehicle (Figure 5E–G). Additional analyses indicate that there was a significant treatment and time interaction ($F_{(1,10)} = 20.825$, $p < 0.001$). Post hoc analysis revealed that NREM sleep time was significantly increased during the dark period by ML297 (Tukey test, $q_{(2)} = 9.159$, $p < 0.001$), but not in the following light period as the drug has a short $t_{1/2}$ (20 min, Figure 5H).

The EEG δ-power or slow-wave activity (SWA) from 0.5 to 4.0 Hz during NREM sleep has been widely used as a measure of sleep intensity. Neither low nor higher dose of ML297 significantly altered the SWA, suggesting that ML297 does not change NREM sleep intensity (Figure 6A). At the 30mg/kg dose, ML297 slightly decreased EEG power during NREM sleep (Figure 6A); however, the alterations are only significant in the α band [main effect, $F(1,10) = 8.082$, $p < 0.02$] and β band [main effect, $F(1,10) = 7.753$, $p < 0.02$], but not in the δ and θ bands. The EEG higher frequencies are often associated with arousal.

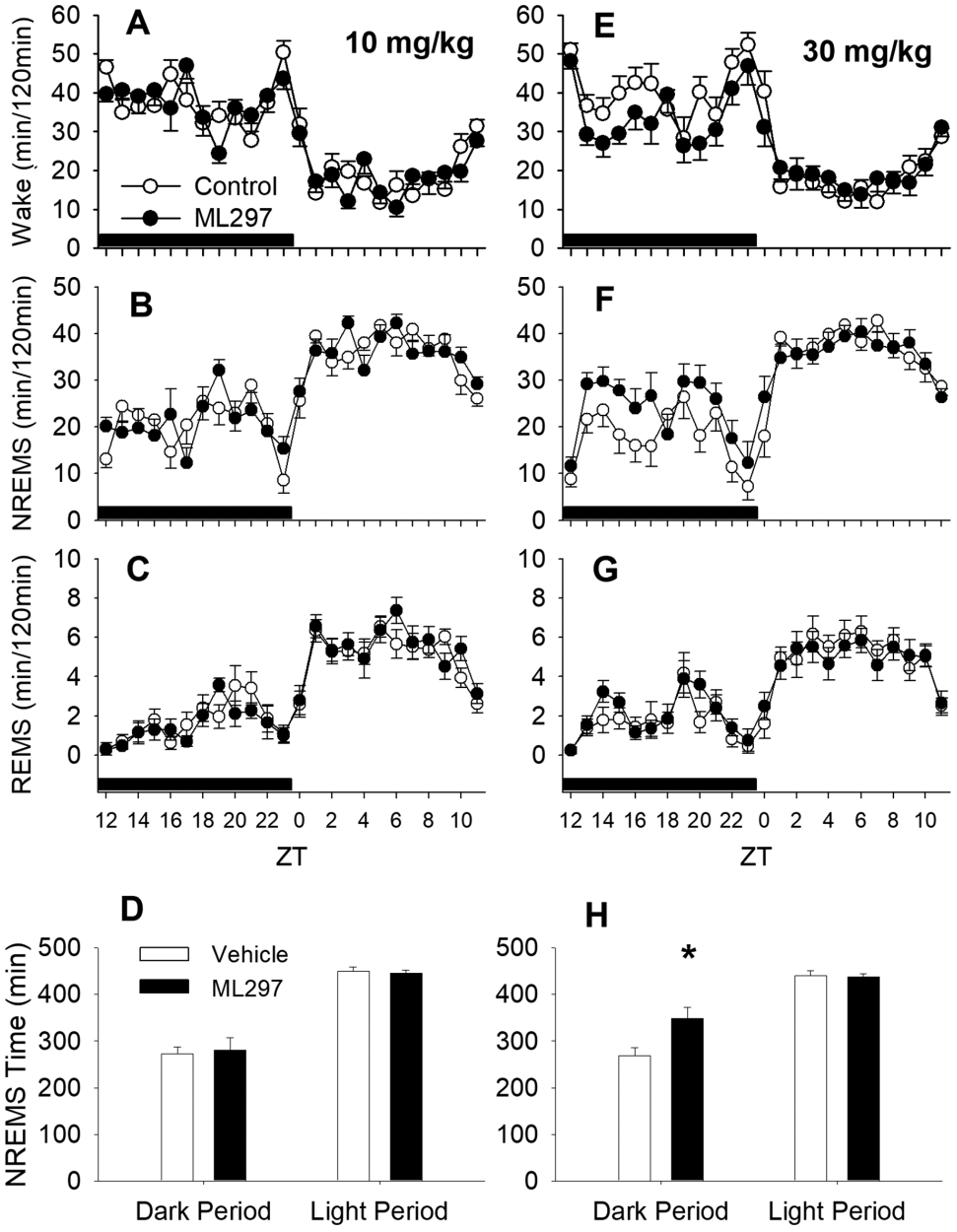

Figure 5. ML297 decreased wakefulness and increased NREM sleep ($n = 6$). At a 10 mg/kg dose, ML297 did not alter the amounts of wakefulness (Wake, A), NREM sleep (NREMS, B), REM sleep (REMS, C). However, at 30 mg/kg, ML297 decreased wakefulness (E) and increased NREMS (F) significantly, but did not alter REMS (G). ML297 at 10 mg/kg had no effect on NREM or REM sleep time during both dark and light periods (D), whereas the higher dose of 30 mg/kg significantly increased NREM sleep time during the dark period (H). The lack of effect during the light phase was due to a short half-life of ML297 (approximately 20 min). Data points/bars and error bars were presented as mean ± SEM. The asterisk indicates significant difference between vehicle and ML297 treatment conditions ($p < 0.05$). The horizontal black bars above x-axis indicate the dark period.

Downloaded from https://academic.oup.com/sleep/article-abstract/42/3/zsy244/5238085 by Law Library user on 06 April 2019

Therefore, the decreases of EEG power in α and β bands suggest that ML297 may help stabilize NREMS by reducing arousal.

Direct GIRK channel activation predominantly promoting NREM sleep is consistent with selective NREM sleep-promoting effects by $GABA_B$ receptor agonists, such as baclofen and GHB [28–31]. However, it is notable that $GABA_B$ receptor overactivation with baclofen or GHB precursor γ-butyrolactone (GBL, which has higher CNS permeability than GHB and can be rapidly converted into GHB in the brain) often induces SWDs in rodents. This is particularly more apparent in rats, whose SWDs resemble human absence seizure activity [32]. Under vehicle control conditions, rat EEG/EMG displayed three vigilant states similar to the mouse (data not shown). ML297 (30 mg/kg, i.p.) prolonged NREM sleep and induced few SWDs. In contrast, R-baclofen (6 mg/kg, i.p.) or GBL (100 mg/kg, i.p.) induced >5 times more SWDs than ML297 (Figure 7E). These SWDs were comprised of

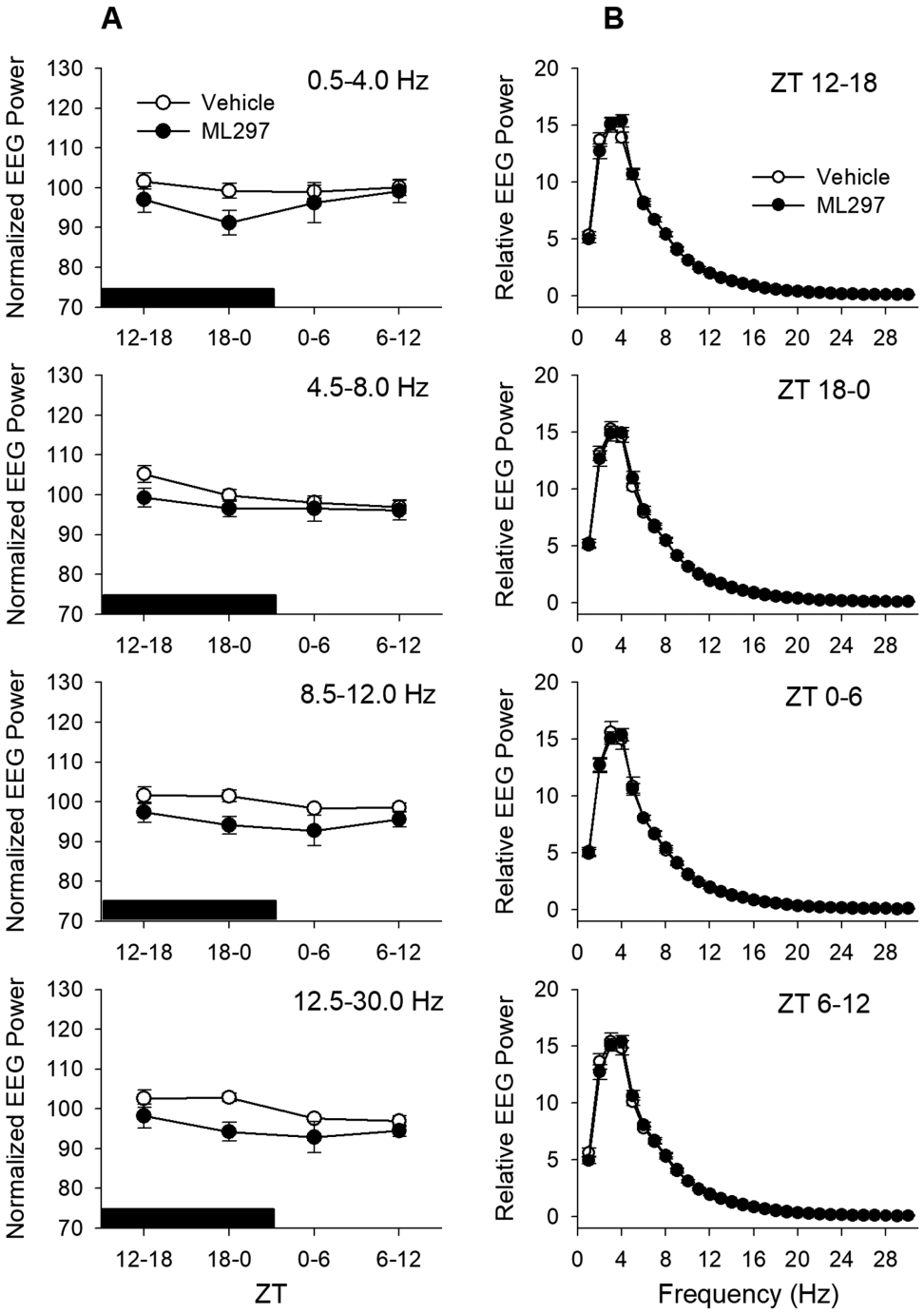

Figure 6. (A) Effects of ML297 on EEG during NREMS were evaluated with power spectral analyses in four frequency bands: δ (0.5–4.0 Hz, or EEG SWA), θ (4.5–8.0 Hz), α (8.5–12.0Hz), and β (12.5–30.0 Hz). The EEG power data during NREMS in each frequency band were normalized for individual animals using average across 24 hr after vehicle injection as 100%. The black bar above the *x*-axis indicates the dark period. There was a slight decrease in EEG power after ML297 treatment, but this decrease was only significant in the α and β bands (see text for statistical details). (B) The relative EEG power from 0.5 to 30.0 Hz is shown as a percent of total power during NREMS.

Downloaded from https://academic.oup.com/sleep/article-abstract/42/3/zsy244/5238085 by Law Library user on 06 April 2019

recurring bursts of special brain electrical waveforms, each of which consists of 4–7 Hz high-amplitude activity lasting for 3–5 s, consistent with the literature [32]. R-baclofen and GBL induced SWDs with short latencies following drug administration (Figure 7F) and lasted for 2 hr or 40 min, respectively.

ML297 does not interfere with fear-conditioned memory and NOR

Finally, current sleep medicines, especially benzodiazepines, frequently cause amnesia, a common side effect leading to a partial inability to recall the recent past. To investigate whether ML297 affects memory, we performed two types of memory tests: fear-conditioned memory and NOR [42, 51]. First, the contextual fear-conditioning test was conducted by re-exposure to the context in which fear was generated with footshocks. The representative mouse movement trajectories before footshock and 24 hr after training are shown in Figure 7A and B, respectively. Conditioned mice exhibited a strong fear response, indicated by reduced traveling distance, movement areas, and specifically freezing behavior. The percentage of time spent in a frozen state prior to training was zero in both groups. Twenty-four hours after training, freezing percentage substantially increased compared with baseline (ANOVA, $p < 0.01$), but there are no significant differences between ML297 and the control group during the 5 min test (13.29 ± 4.86% in the ML297 group vs 13.54 ± 3.56% in control, post hoc PLSD between the two groups, $p > 0.05$; Figure 8C).

Following completion of the contextual test, the tone-conditioned fear test was immediately performed. The representative mouse movement trajectories before, during, and after the delivery of conditioned stimuli of 5 tones are shown

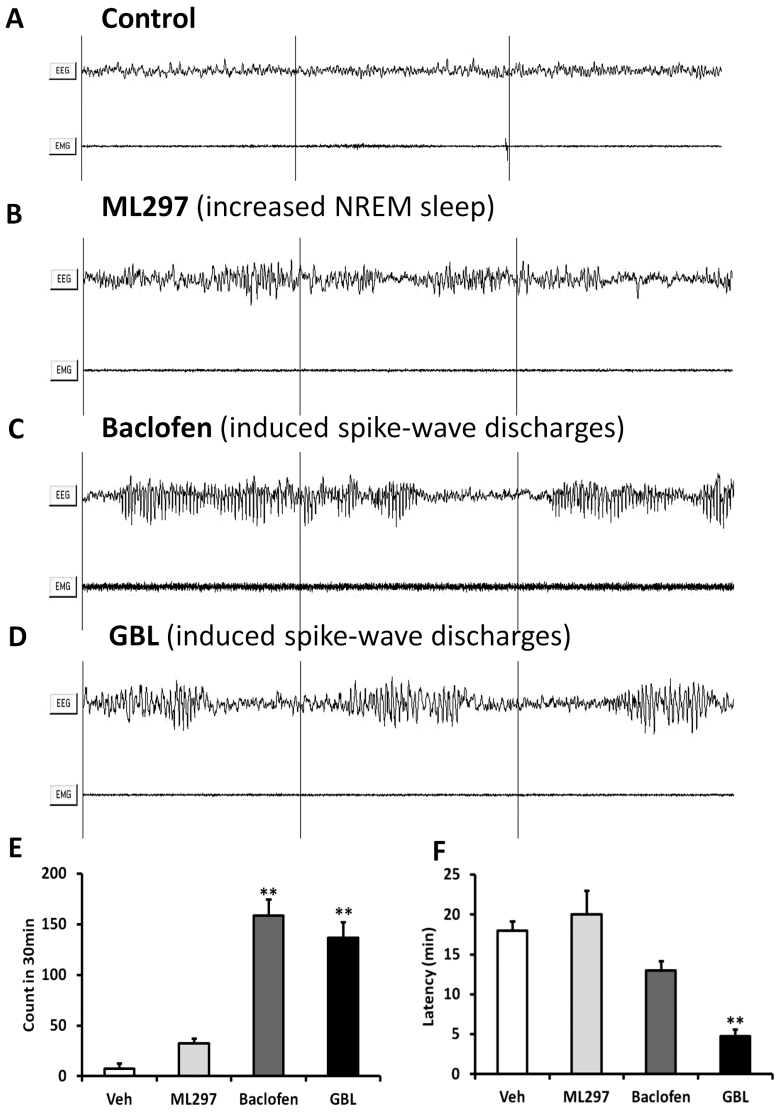

Figure 7. GIRK channel direct activation induced fewer SWDs compared with $GABA_B$ receptor activation. (A) EEG/EMG recording traces of wakefulness of a control rat injected with the vehicle in the dark phase. (B) ML297 (30 mg/kg, i.p.) promoted NREM sleep without inducing SWDs during the dark phase. (C) In the same animal, R-baclofen (6 mg/kg, i.p.) rapidly induced multiple SWDs, each of which consists of 4–7 Hz high-amplitude brain electrical waveforms lasting for 3–5 s. Recurrance of SWDs lasted for approximately 2 hr following the drug administration. (D) γ-butyrolactone (GBL (100 mg/kg, i.p.) caused SWDs approximately 15 min following drug administration and lasted for 40–50 min. (E) Comparison of SWD episodes (number/30 min) among baclofen, GBL, ML297, and vehicle from pooled data ($n = 6$, ANOVA followed by post hoc PLSD test between drug and vehicle, $^{**}p < 0.01$). (F) Summary of latencies to the first SWD episode among baclofen, GBL, ML297, and vehicle from pooled data ($n = 6$, ANOVA followed by post hoc PLSD test between drug and vehicle, $^{**}p < 0.01$).

Downloaded from https://academic.oup.com/sleep/article-abstract/42/3/zsy244/5238085 by Law Library user on 06 April 2019

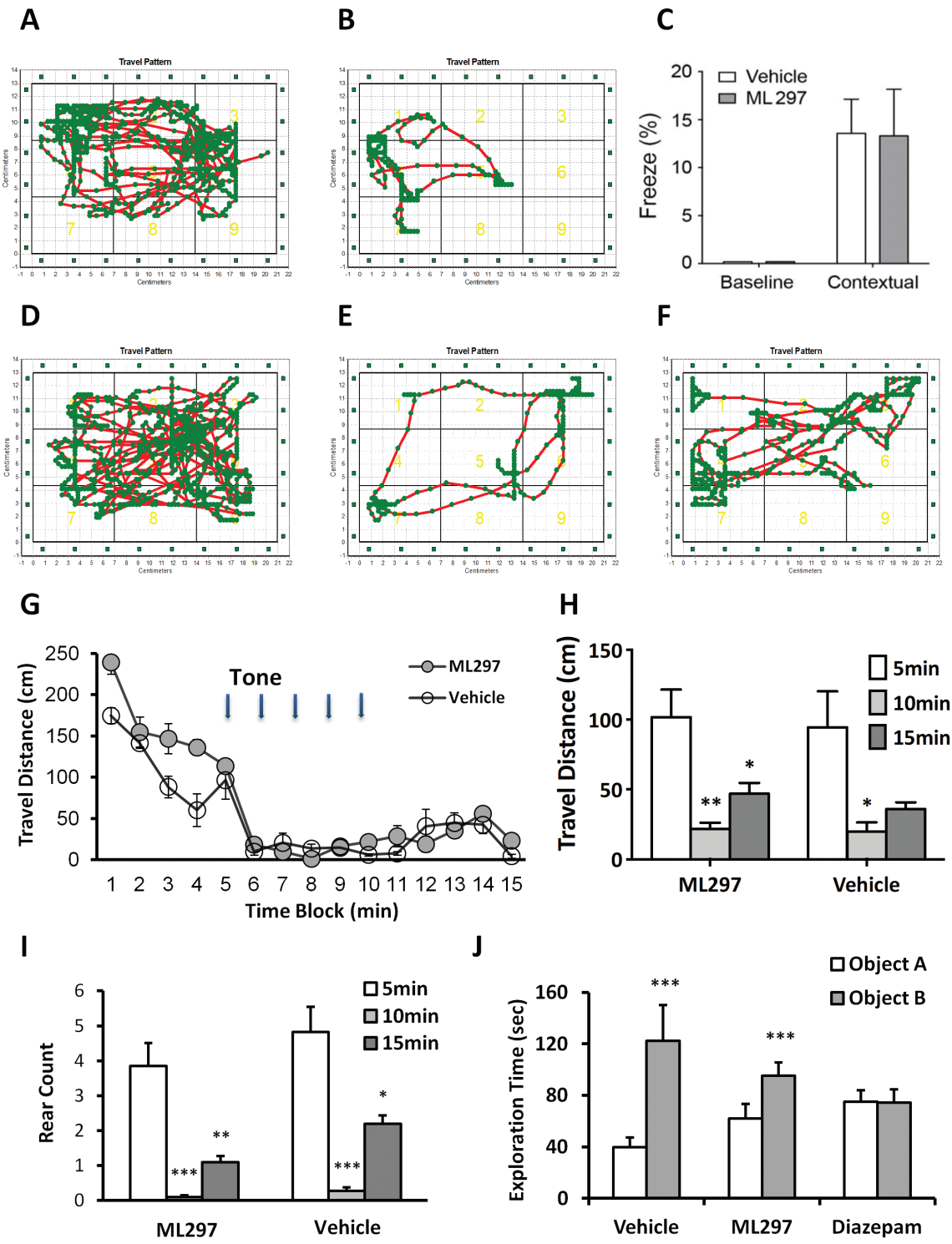

Figure 8. Direct activation of GIRK channels with ML297 does not cause impairment of fear-conditioned responses, and novel object recognition. (A) In the contextual fear conditioning test, representative mouse moving trajectories prior to footshock in the training day are shown. (B) Twenty-four hours after footshocks (training) with subsequent re-exposure to context are shown in (A) and (B), respectively. (C) Freezing % in baseline and contexual-conditioned under ML297 (30 mg/kg, i.p.) treatment or vehicle condition was plotted. There are sigificant differences in contexual freezing time compared with baseline but insigficant differences between ML297 and control groups (ANOVA, $p < 0.01$ among the four groups; post hoc PLSD between two treatment groups, $p > 0.05$, $n = 8$/group). The representative mouse moving trajectories before, during, and after 5-tone is shown in (D), (E), and (F), respectively. (G–H) Time courses of traveling distance in 1 min bins indicate that tones dramatically decreased locomotion with partial recovery. (I) Averaged rearing activity counts are shown in the histogram before, during, and after 5-tone under ML297 or vehicle treatment conditions. (ANOVA, $p < 0.05$ among the six conditions; post hoc PLSD between two treatment groups, $p > 0.05$, $n = 8$/group). (J) Ability of novel object recognition was quantified by the % exploring time spent toward the novel object over total exploring time toward the familiar (A) and novel objects (B) under ML297 (30 mg/kg, i.p.), diazepam (3 mg/kg, i.p.), or vehicle treatment conditions at 24 hr after the training ($n = 8$/group, ANOVA, $p < 0.01$ among the six conditions; post hoc PLSD between exploring A and B objects, $^{***}p > 0.001$). Total exploring time toward two identical objects on training session and on test session toward the familiar (A) and novel objects (B) under ML297, diazepam, or vehicle treatment conditions at 24 hr after the training ($n = 8$/group, ANOVA, $p = 0.14$ among the six conditions).

Downloaded from https://academic.oup.com/sleep/article-abstract/42/3/zsy244/5238085 by Law Library user on 06 April 2019

in Figure 8D–F, respectively, indicating that tones significantly and reversibly reduced movement areas. The time course (Figure 8G) and three time blocks (Figure 8H) of travel distance quantitatively indicate that tones significantly and reversibly reduced traveling distance. Concurrently, tone-cued fear conditioning responses almost completely depressed rearing activity as quantified by rearing count (Figure 8I; ANOVA, $p < 0.01$).

To complement the fear conditioning testing, the NOR test was conducted. Both randomly assigned groups of mice exhibited similar levels of object exploration in an open field chamber. Both control and ML297 (30 mg/kg, i.p.) showed significant increases in exploration time of a novel object, indicating that ML297 does not impair NOR at 24 hr after training (Figure 8J). In contrast, mice treated with diazepam (3 mg/kg, i.p.) spent an equal amount of time in exploring the familiar and novel objects, indicating a complete loss of NOR ability.

Discussion

In the present study, we have found that, at the cellular level, the small molecule GIRK channel activator ML297 causes long-lasting postsynaptic inhibition on both hypothalamic hypocretin and hippocampal pyramidal neurons without significant depression of neurotransmission (e.g. EPSCs/IPSCs); at the whole organism level, ML297 reduces wakefulness, locomotor activity, and preferentially increases NREM sleep time without altering NREM sleep intensity and REM sleep. Moreover, ML297 does not cause SWDs nor impairs fear conditioned memory or NOR. For the first time, we have provided direct evidence for the role of neuronal GIRK channels in the regulation of neuronal excitability and wake/sleep state. Consequently, direct activation of GIRK channels can provide a new approach in developing sleep-promoting therapeutics.

Several studies have shown that functional GIRK channels in hypocretin neurons are activated by multiple endogenous neurotransmitters such as GABA via $GABA_B$ receptors [45] and 5-HT via activation of $5\text{-}HT_{1A}$ receptors [35]. They can also be modulated by neuropeptides such as nociceptin/orphanin FQ (N/OFQ) through NOP receptors [36]. The hippocampal pyramidal neurons are well-defined to express abundant GIRK1/2 channels [52, 53] and its functional modulation by a variety of metabotropic receptors ($GABA_B$, metabotropic glutamate receptors, muscarinic, adenosine A1, opioid μ receptors, etc.) has been documented [54, 55]. In this study, we have shown that ML297 directly opens the same GIRK channel that is activated by these neurotransmitters and modulators. The concentration-dependent hyperpolarization response revealed an EC_{50} (5.4 μM) of ML297 in hypocretin neurons about 10-fold higher than its EC_{50} (0.5 μM) determined from recombinant GIRK1/2 channels expressed in HEK293 cells [24, 40]. The potency discrepancy is not unusual in brain slice studies and could be due to limitation of target access in a thicker tissue compared with a single layer of cultured cells. Interestingly, ML297 activation of GIRK channels selectively produces postsynaptic inhibition with little effect on presynaptic neurotransmission.

The GIRK channel subunit compositional diversity, heterogeneous distribution, principal expression in excitatory neurons, predominant expression on the postsynaptic membrane, and different sensitivities to ML297 provide a molecular and neuroanatomic basis for a differential pharmacological modulation of neuronal excitability. The systemic consequences of activation of GIRK channels could manifest in different behavioral endpoints and may have the potential for a range of indications. The activation of GIRK channels with ML297 in hypocretin neurons may result in tuning down of this wake-promoting system. While in hippocampal pyramidal neurons, ML297 can alter alertness, cognitive function, and indirectly promote sleep. ML297's effects on GIRK channels expressed in other types of neurons, particularly cortical neurons, would also greatly contribute to its sleep-promoting action. In addition, ML297 has shown anticonvulsant activity in mice induced by either pentylenetetrazole or electric shock [24, 56], and anxiolytic effects on anxiety-like behavior in mice [40].

It has been observed that baclofen and the GHB precursor GBL often cause SWDs in addition to increasing NREM sleep. The SWD resembles human absence seizure activity and has been suggested to be a model of childhood absence epilepsy [32–34]. Although the mechanism of SWD generation is elusive, direct activation of GIRK channels with ML297 avoids the induction of SWDs which could translate into fewer unwanted side effects in future clinical applications. Finally, unlike commonly used insomnia medications such as benzodiazepines, direct activation of GIRK channels apparently does not impair contextual memory, a hippocampus-dependent memory, nor tone-conditioned retention, which is thought to be a hippocampus-independent memory. Furthermore, ML297 did not impair NOR, which is also a hippocampus-dependent memory test. Taken together with the contextual- and tone-fear conditioning tests, these studies indicate that, unlike diazepam, ML297 at sleep-promoting doses does not cause impairment in memory.

In summary, insomnia is a major health problem affecting a significant percentage of the population worldwide. Current medications for insomnia are limited by side effects, tolerance, and addictive liabilities. Direct GIRK channel activation presents a new mechanism of action and a strategy for inhibiting the excitatory arousal system as opposed to potentiating the inhibitory sleep system to treat insomnia. If future studies demonstrate that tolerance does not develop from chronic use of a GIRK channel activator and a lack of liability in drug dependence, which are major concerns with benzodiazepines and GHB, then a GIRK channel activator would provide a more effective and safer approach in the treatment of chronic insomnia and potentially other neurological disorders caused by neuronal hyperactivity.

Acknowledgments

Permission for use of the orexin/EGFP mice was kindly given by Dr. Takeshi Sakurai, Kanazawa University School of Medicine. The transgenic mice were initially bred in SRI International and kindly provided by Dr. T. Kilduff. A batch of ML297 was synthesized and kindly provided by Dr. Heike Wulff, University of California, Davis. Zhaohui Li, PhD candidate at UCLA, and Eric Shen, undergraduate at UC Berkeley, were interns and provided technical assistance.

Funding

This work was supported by National Institutes of Health grants: R43 HL142315, R42 HL084990, R44 AG043203, and R44 NS086343.

Downloaded from https://academic.oup.com/sleep/article-abstract/42/3/zsy244/5238085 by Law Library user on 06 April 2019

Conflict of interest statement. The SmartCage system with CageScore software developed by AfaSci, Inc. was used to monitor animal active/inactive state, locomotion, perform rotarod test, and conduct contextual and tone-conditioning fear test in this study. X. Xie is the founder and owner of AfaSci. The SleepWave software was developed by Biosoft Studio which was used for EEG/GMG recordings. J. Fang is the owner of Biosoft Studio.

References

1. Morin CM, *et al*. Chronic insomnia. *Lancet*. 2012;**379**(9821):1129–1141.
2. Kaczor M, *et al*. Prevalence and consequences of insomnia in pediatric population. *Psychiatr Pol*. 2016;**50**(3):555–569.
3. Lane JM, *et al*. Genome-wide association analyses of sleep disturbance traits identify new loci and highlight shared genetics with neuropsychiatric and metabolic traits. *Nat Genet*. 2017;**49**(2):274–281.
4. Angarita GA, *et al*. Sleep abnormalities associated with alcohol, cannabis, cocaine, and opiate use: a comprehensive review. *Addict Sci Clin Pract*. 2016;**11**(1):9.
5. McCleery J, *et al*. Pharmacotherapies for sleep disturbances in dementia. *Cochrane Database Syst Rev*. 2016;**11**:CD009178.
6. Porter VR, *et al*. Sleep, cognition and dementia. *Curr Psychiatry Rep*. 2015;**17**(12):97.
7. Rodrigues TM, *et al*. Pharmacological interventions for daytime sleepiness and sleep disorders in Parkinson's disease: systematic review and meta-analysis. *Parkinsonism Relat Disord*. 2016;**27**:25–34.
8. Gilbert KS, *et al*. Sleep disturbances, TBI and PTSD: implications for treatment and recovery. *Clin Psychol Rev*. 2015;**40**:195–212.
9. Osorio RS, *et al*. Greater risk of Alzheimer's disease in older adults with insomnia. *J Am Geriatr Soc*. 2011;**59**(3):559–562.
10. Kang JE, *et al*. Amyloid-beta dynamics are regulated by orexin and the sleep-wake cycle. *Science*. 2009;**326**(5955):1005–1007.
11. Vandrey R, *et al*. Interactions between disordered sleep, posttraumatic stress disorder, and substance use disorders. *Int Rev Psychiatry*. 2014;**26**(2):237–247.
12. Coffey AA, *et al*. Reversal of the sleep-wake cycle by heroin self-administration in rats. *Brain Res Bull*. 2016;**123**:33–46.
13. Brower KJ, *et al*. Prevalence and correlates of withdrawal-related insomnia among adults with alcohol dependence: results from a national survey. *Am J Addict*. 2010;**19**(3):238–244.
14. Maulik PK, *et al*. Coping behaviors and relapse precipitants in opioid dependence: a study from North India. *J Subst Abuse Treat*. 2002;**22**(3):135–140.
15. Raj H, *et al*. Relapse precipitants in opiate addiction: assessment in community treatment setting. *Indian J Psychiatry*. 2000;**42**(3):253–257.
16. Brannan SK, *et al*. Duloxetine 60 mg once-daily in the treatment of painful physical symptoms in patients with major depressive disorder. *J Psychiatr Res*. 2005;**39**(1):43–53.
17. Brown MA, *et al*. A review of sodium oxybate and baclofen in the treatment of sleep disorders. *Curr Pharm Des*. 2011;**17**(15):1430–1435.
18. Richey SM, *et al*. Pharmacological advances in the treatment of insomnia. *Curr Pharm Des*. 2011;**17**(15):1471–1475.
19. Scarff JR. Suvorexant for Adults with Insomnia. *J S C Med Assoc*. 2015;**111**(1):28–29.
20. Owen RT. Suvorexant: efficacy and safety profile of a dual orexin receptor antagonist in treating insomnia. *Drugs Today (Barc)*. 2016;**52**(1):29–40.
21. Sutton EL. Profile of suvorexant in the management of insomnia. *Drug Des Devel Ther*. 2015;**9**:6035–6042.
22. Szabadi E. Selective targets for arousal-modifying drugs: implications for the treatment of sleep disorders. *Drug Discov Today*. 2014;**19**(5):701–708.
23. Monti JM, *et al*. Zolpidem's use for insomnia. *Asian J Psychiatr*. 2017;**25**:79–90.
24. Kaufmann K, *et al*. ML297 (VU0456810), the first potent and selective activator of the GIRK potassium channel, displays antiepileptic properties in mice. *ACS Chem Neurosci*. 2013;**4**(9):1278–1286.
25. Logothetis DE, *et al*. Unifying mechanism of controlling kir3 channel activity by g proteins and phosphoinositides. *Int Rev Neurobiol*. 2015;**123**:1–26.
26. Logothetis DE, *et al*. Gating of G protein-sensitive inwardly rectifying K+ channels through phosphatidylinositol 4,5-bisphosphate. *J Physiol*. 1999;**520 Pt 3**:630.
27. Xie X, *et al*. gamma-Hydroxybutyrate depresses monosynaptic excitatory and inhibitory postsynaptic potentials in rat hippocampal slices. *Eur J Pharmacol*. 1992;**223**(2-3):193–196.
28. Black J, *et al*. The nightly administration of sodium oxybate results in significant reduction in the nocturnal sleep disruption of patients with narcolepsy. *Sleep Med*. 2009;**10**(8):829–835.
29. Black J, *et al*. Impact of sodium oxybate, modafinil, and combination treatment on excessive daytime sleepiness in patients who have narcolepsy with or without cataplexy. *Sleep Med*. 2016;**24**:57–62.
30. Black SW, *et al*. GABAB agonism promotes sleep and reduces cataplexy in murine narcolepsy. *J Neurosci*. 2014;**34**(19):6485–6494.
31. Roth T, *et al*. Effect of sodium oxybate on disrupted nighttime sleep in patients with narcolepsy. *J Sleep Res*. 2017;**26**(4):407–414.
32. Snead OC 3rd. Evidence for GABAB-mediated mechanisms in experimental generalized absence seizures. *Eur J Pharmacol*. 1992;**213**(3):343–349.
33. Stewart LS, *et al*. Severity of atypical absence phenotype in GABAB transgenic mice is subunit specific. *Epilepsy Behav*. 2009;**14**(4):577–581.
34. Ostojić ZS, *et al*. GABAB receptors as a common target for hypothermia and spike and wave seizures: intersecting mechanisms of thermoregulation and absence epilepsy. *Neuroscience*. 2013;**238**:39–58.
35. Muraki Y, *et al*. Serotonergic regulation of the orexin/hypocretin neurons through the 5-HT1A receptor. *J Neurosci*. 2004;**24**(32):7159–7166.
36. Xie X, *et al*. Hypocretin/orexin and nociceptin/orphanin FQ coordinately regulate analgesia in a mouse model of stress-induced analgesia. *J Clin Invest*. 2008;**118**(7):2471–2481.
37. Khroyan TV, *et al*. Rodent motor and neuropsychological behaviour measured in home cages using the integrated modular platform SmartCage™. *Clin Exp Pharmacol Physiol*. 2012;**39**(7):614–622.
38. Fang J, *et al*. Mice lacking the TNF 55 kDa receptor fail to sleep more after TNFalpha treatment. *J Neurosci*. 1997;**17**(15):5949–5955.
39. Dudhgaonkar SP, *et al*. Synergistic interaction between meloxicam and aminoguanidine in formalin-induced nociception in mice. *Eur J Pain*. 2008;**12**(3):321–328.

Downloaded from https://academic.oup.com/sleep/article-abstract/42/3/zsy244/5238085 by Law Library user on 06 April 2019

40. Wydeven N, *et al*. Mechanisms underlying the activation of G-protein-gated inwardly rectifying K+ (GIRK) channels by the novel anxiolytic drug, ML297. *Proc Natl Acad Sci USA*. 2014;**111**:10755–10760.
41. Kotecki L, *et al*. GIRK channels modulate opioid-induced motor activity in a cell type- and subunit-dependent manner. *J Neurosci*. 2015;**35**(18):7131–7142.
42. Radulovic J, *et al*. Generalization of fear responses in C57BL/6N mice subjected to one-trial foreground contextual fear conditioning. *Behav Brain Res*. 1998;**95**(2):179–189.
43. Hicks JA, *et al*. Voluntary wheel-running attenuates insulin and weight gain and affects anxiety-like behaviors in C57BL6/J mice exposed to a high-fat diet. *Behav Brain Res*. 2016;**310**:1–10.
44. Lueptow LM. Novel object recognition test for the investigation of learning and memory in mice. *J Vis Exp*. 2017;**126**:e55718. doi:10.3791/55718.
45. Xie X, *et al*. GABA(B) receptor-mediated modulation of hypocretin/orexin neurones in mouse hypothalamus. *J Physiol*. 2006;**574**(Pt 2):399–414.
46. Ladera C, *et al*. Pre-synaptic GABA receptors inhibit glutamate release through GIRK channels in rat cerebral cortex. *J Neurochem*. 2008;**107**(6):1506–1517.
47. Sarvey JM, *et al*. Long-term potentiation: studies in the hippocampal slice. *J Neurosci Methods*. 1989;**28**(1-2):109–124.
48. Thompson SM, *et al*. Comparison of the actions of adenosine at pre- and postsynaptic receptors in the rat hippocampus in vitro. *J Physiol*. 1992;**451**:347–363.
49. Qu W, *et al*. Automated monitoring of early neurobehavioral changes in mice following traumatic brain injury. *Neural Regen Res*. 2016;**11**(2):248–256.
50. Rajasekaran N, *et al*. Reduced locomotor activity correlates with increased severity of arthritis in a mouse model of antibody-induced arthritis. *Open J Rheumat Autoimmune Dis*. 2014;**4**:62–68.
51. Shoji H, *et al*. Contextual and cued fear conditioning test using a video analyzing system in mice. *J Vis Exp*. 2014;**85**:e50871. doi:10.3791/5087.
52. Harashima C, *et al*. Abnormal expression of the G-protein-activated inwardly rectifying potassium channel 2 (GIRK2) in hippocampus, frontal cortex, and substantia nigra of Ts65Dn mouse: a model of Down syndrome. *J Comp Neurol*. 2006;**494**(5):815–833.
53. Marron Fernandez de Velasco E, *et al*. GIRK2 splice variants and neuronal G protein-gated K+ channels: implications for channel function and behavior. *Scientific reports*. 2017;**7**:1639.
54. Yi BA, *et al*. Controlling potassium channel activities: interplay between the membrane and intracellular factors. *Proc Natl Acad Sci USA*. 2001;**98**:11016–11023.
55. Nagi K, *et al*. Kir3 channel signaling complexes: focus on opioid receptor signaling. *Front Cell Neurosci*. 2014;**8**:186.
56. Huang Y, *et al*. GIRK1-mediated inwardly rectifying potassium current suppresses the epileptiform burst activities and the potential antiepileptic effect of ML297. *Biomed Pharmacother*. 2018;**101**:362–370.

Downloaded from https://academic.oup.com/sleep/article-abstract/42/3/zsy244/5238085 by Law Library user on 06 April 2019